Enclosure #2
Final Technical Report
USAF GR AFOSR 91-0333

THE ACTIVITY OF HIGH-FREQUENCY VIBRATORY SENSITIVE NEURONS IN MONKEY PRIMARY SOMATOSENSORY CORTEX DURING THE INITIATION OF VIBRATORY AND VISUALLY CUED HAND MOVEMENTS

Michael A. Lebedev and Randall J. Nelson

Department of Anatomy and Neurobiology

University of Tennessee, Memphis

875 Monroe Avenue, Memphis, TN 38163

Telephone: (901) 448 5979

FAX: (901) 448 7193

E-mail: rnelson@utmem1.utmem.edu

Abstract

The activity of high-frequency vibratory sensitive (HFVS) neurons was recorded in monkey primary somatosensory cortex (SI) while animals performed wrist flexions and extensions in response to 27, 57 or 127 Hz palmar vibration or in response to visual stimuli serving as go-cues. HFVS neurons were distinguished by their best responsiveness to the highest frequency vibration (127 Hz) being better than to the lower frequencies. These neurons probably received input from Pacinian afferents. HFVS neurons formed a unique population that constituted ~4 % of the task-related cells, and more frequently were found in areas 3b and 1 (5.3% and 5.4% of the cells recorded in these areas, respectively) than in areas 3a or 2 (1.1% and 2.5%, respectively). Both vibration-entrained and non-entrained HFVS neurons were observed. Discharges of entrained neurons were distributed non-uniformly over the vibratory cycle. In addition, these neurons were characterized by multimodal distributions of interspike intervals and negative serial correlations in joint interval scatterplots. Entrained neurons responded to vibration at shorter latencies and with higher firing rates (17.6 ± 4.3 ms and 123 ± 40 spikes / s, respectively, during 127 Hz vibration) than non-entrained neurons (23.9 ± 7.5 ms and 84 ± 44 spikes / s). These observations are consistent with the suggestion that entrained and non-entrained HFVS neurons belong to hierarchical stages of information processing. For these neurons, movement-associated changes in activity occurred earlier than movement onset, but, in most instances (~80%), occurred later than the onset of electromyographic activity of forearm muscles. Therefore, these activity changes could result from peripheral inputs. However, movement-associated changes in activity were different during vibratory and visually cued trials. During vibratory cued trials, firing rates of HFVS neurons typically decreased prior to the onsets of both flexion and extension movements. However, during visually-cued trials, premovement increases in firing rates occurred more frequently. We suggest that premovement modulation of the vibratory responsiveness of HFVS neurons may result from central gating of somatosensory information rather than mere replication of changes in peripheral inputs.

Key words: somatosensory cortex, high-frequency vibrotactile stimulation, stimulus-entrained activity, Pacinian afferent.

Introduction

Somatosensory afferent fibers of different submodalities (slowly adapting, rapidly adapting and Pacinian afferents) are preferentially sensitive to the vibratory stimulation in characteristic frequency ranges (Talbot et al. 1968). Pacinian afferents are preferentially activated by high-frequency (80-400 Hz) vibration (Sato 1961; Talbot et al. 1968). During high-frequency vibratory stimulation, the responses of Pacinian afferents are commonly entrained to the stimulus frequency (Sato 1961; Talbot et al. 1968). However, precision of entrainment of neuronal activity to vibration declines, as the signals from Pacinian afferents ascend to cortical levels (Burton and Sinclair 1991; Ferrington and Rowe 1980; Mountcastle et al. 1969). In primary somatosensory cortex (SI), only a portion of high-frequency vibratory sensitive (HFVS) neurons is vibration-entrained (Ferrington and Rowe 1980; Mountcastle et al. 1969). Mountcastle and coworkers (1969) suggested that the predominant inputs to vibration-entrained SI neurons are from direct thalamocortical projections, whereas non-entrained SI neurons receive higher-order intracortical projections. Thus, these subpopulations of entrained and non-entrained SI neurons may belong to different hierarchical stages of information processing.

To elucidate the functional role of entrained and non-entrained HFVS SI neurons role during motor behavior, we examined their activity recorded in monkeys while the animals performed vibratory and visually cued wrist movements. Studies of behaving animals have increased our understanding of the possible roles of SI neurons in the control of voluntary movements (for review, see Nelson 1988). The specific role of HFVS neurons in motor control, however, is poorly understood. We sought to determine the firing patterns of HFVS neurons that were associated with the onsets of go-cues and movements. To distinguish between vibration-entrained and non-entrained subpopulations of SI neurons, temporal characteristics of neuronal responses to vibration were examined using spike train analysis methods (Mountcastle et al. 1969; 1990; Perkel et al. 1967; Poggio and Viernstein 1964; Rodieck et al. 1962; Surmeier and Towe 1987a; 1987b). We found differences in the activity patterns of entrained and non-entrained HFVS neurons, as well as differences in the activity patterns recorded for each group during the vibratory and visually cued trials. Some of these data have been presented previously in preliminary form (Lebedev and Nelson 1994).

Methods

Experimental Apparatus and Behavioral Paradigm

Four adult male rhesus monkeys (*Macaca mulatta*; monkeys F, G, H and N) were trained to make wrist flexions and extensions in response to vibrotactile and visual go-cues. The monkeys were cared for in accordance with the *NIH Guide for Care and Use of Laboratory Animals,* revised 1985. The experimental apparatus and behavioral paradigm have been described in detail elsewhere (Nelson 1988; Nelson et al. 1991). Briefly, each animal sat in an acrylic monkey chair with its right forearm on an armrest and its right palm on a moveable plate. One end of the plate was attached to the axle of a brushless DC torque motor (Colburn and Evarts 1978). A load of 0.07 Nm was applied to the plate, which assisted wrist extensions and opposed flexions. Feedback of current wrist position was provided by a visual display located 35 cm in front of an animal. This visual display consisted of 31 light-emitting diodes (LEDs). The middle, red LED corresponded to a centered wrist position. Yellow LEDs above and below the middle LED indicated successive angular deviations of 1°. An instructional, red LED was located in the upper left corner of the visual display.

A trial began when the monkey centered the plate. At this time, a movement direction request was given by the instructional LED. If this LED was illuminated, the appropriate movement was extension. Otherwise, flexion was requested. The monkey was required to hold the plate in the centered position until a go-cue was presented. Movements of more than 0.5° from the center position during this hold period canceled a trial. After the center position was held for the required time (0.5, 1.0, 1.5, or 2.0 s; pseudorandomized), a vibratory or a visual go-cue was presented. During vibratory cued trials, the plate was vibrated by driving the torque motor with a sine wave that caused angular deflection of less than 0.06° resulting in plate movement of less than 100 μm peak-to-peak measured 10 cm distal to the coupling of the handle to the motor. The motor was driven at 27, 57, and 127 Hz in different blocks of trials. The onset of vibratory stimulation signaled the monkey that he could make a movement. During visually cued trials, animals initiated movements in response to shifts of the position indicator from the center position. The shift corresponded to a 5° deviation in the opposite direction from the requested movement. The shift was produced by adding a DC voltage to the wrist position signal. During both vibratory and

visually cued trials, go-cues remained on until a movement of at least 5° in the required direction was made. Then go-cues were turned off, and the animal received a fruit juice reward. A new trial began when an animal once again centered the plate.

Electrophysiological Recordings and Histology

A stainless steel recording chamber was surgically implanted in order to make extracellular recordings of the activity of SI neurons (see Nelson et al. 1991, for details). The recordings were performed using platinum-iridium microelectrodes. Transdural penetrations were made daily into the contralateral hand representation. The activity of single neurons was amplified, and converted into pulse data with a time-amplitude window discriminator (Evarts 1966; Lemon 1984; Nelson 1988; Nelson et al. 1991). Neuronal receptive fields (RFs) were examined by lightly touching skin surfaces, manipulating joints, and palpating muscles. In a series of experiments, the electromyographic (EMG) activity of forearm muscles acting across the wrist was recorded using intramuscular EMG wires (Nelson 1987). EMG activity was converted into pulse data (Vaadia et al. 1988; Nelson 1987).

On the last recording day, electrolytic lesions were made in the cortex by passing the current of 10 μA through a recording electrode for 10-20 s. These lesions provided references for histological reconstruction of the recording sites. The animals were then deeply anesthetized with sodium pentobarbital and transcardially perfused with 10% buffered formol-saline. Histological sections of the cortex were prepared, and recording sites were reconstructed based upon the location of electrode penetrations in sagittal sections relative to marking lesions and the depth from the cortical surface (Fig. 1) (Nelson 1988; Nelson et al. 1991).

Figure 1 About Here

Spike Train Analyses

Neurons were classified as HFVS if they exhibited higher firing rates during 127 Hz vibratory stimulation than during 27 and 57 Hz stimulation. Spike train analyses were performed to distinguish between vibration-entrained and non-entrained neurons. Neurons were considered vibration-entrained if their discharges were distributed non-uniformly over the vibratory cycle (Mountcastle et al., 1969). The occurrences of discharges relative to the vibratory cycle were represented by phase raster displays that showed, for each spike, the time of its occurrence on the x-axis and the phase relative to the vibratory cycle on the y-axis (Fig. 2F) (Lebedev et al. 1994). In addition, histograms were constructed for the distributions of discharges over vibratory cycles (Fig. 4C&F). For vibration-entrained activity, phase rasters and cycle distribution histograms indicated the phase of the stimulus cycle at which neuronal responses preferentially occurred (Fig. 2F and Fig. 4C, respectively). For non-entrained neurons, the phases of individual spikes were scattered randomly within graph limits (Fig. 3F and Fig. 4F, respectively). Additional information about the characteristics of entrainment of neuronal activity to vibration was provided by ISI histograms. During vibratory entrainment, ISIs preferentially occurred near multiples of the vibratory period (Fig. 4A) (Mountcastle et al. 1969; Talbot et al. 1968). To examine this, ISI histograms were analyzed for the presence of peaks at multiples of the vibratory period. The spike train analyses were done to examine serial dependencies of ISIs by using joint interval scattergrams, which are plots that show the relationship between immediately adjacent ISIs (Rodieck et al. 1962; Siebler et al. 1991; Surmeier and Towe 1987a; 1987b).

Figure 2 About Here

Changes of neuronal activity that occurred during the performance of the task were illustrated using multi-panel displays (Fig. 2E-F). Each of the panels contained records centered on cue onset or movement onset (left or right parts, respectively). The displays included conventional discharge histograms (Fig. 2B) and raster plots (Fig. 2C). In addition, ISI rasters were plotted that displayed the time of occurrence of each spike on the x-axis and that of the succeeding ISI on the y-axis (Fig. 2A) (Wall and Cronly-Dilon 1960). The onsets of changes in neuronal firing rate and of changes in EMG were determined using cumulative sum (CUSUM) methods (Ellaway 1977; Jiang et al. 1991). The CUSUM at a given time was calculated as the total number of discharges accumulated for all trials from some starting time. The CUSUM was then rescaled by dividing it by the total number of trials, so that the slope of the derived average CUSUM provided a measure of the neuron's firing rate (Fig. 2D). To calculate the onset of firing rate changes, the largest epoch of near-linear rise in the average CUSUM occurring prior to a behaviorally significant event was labeled by visual inspection. This epoch typically was ~200 ms. The CUSUM for this epoch was fitted by a linear least-squares interpolation curve. The standard deviation of the CUSUM from the interpolation curve was calculated. The interpolation curve was then extrapolated through the epoch containing the event. A computer program searched forward in time to find the first change in the CUSUM from the curve of more than three standard deviations for at least 40 ms. The time at which the CUSUM varied from the predicted value was designated as the onset of a significant change in activity.

Figure 3 About Here

The characteristics of activity of the studied neurons were statistically analyzed using a multifactorial ANOVA (with the Scheffé post hoc test). Both parametric (*t*-test) and nonparametric (Mann-Whitney *U*-test) statistics were used for two group comparisons.

Results

Database

Of the total recorded 808 task-related SI neurons recorded from the four monkeys, 32 high-frequency vibratory sensitive (HFVS) neurons (4.0%) were selected. Twenty eight neurons were tested for receptive fields (RFs). Of these, 20/28 neurons had receptive fields (RFs) located on the palmar surface of the hand. These neurons probably received inputs from Pacinian corpuscles of the dermal and subcutaneous types (Cauna and Mannan 1958; Sato 1957; Kumamoto et al. 1993). Four neurons were activated by passively manipulating joints. These neurons may have received inputs from the Pacinian afferents located in the connective tissue of joints or muscles (Quilliam 1966). For four neurons, no clear RFs were found. The distribution of cortical locations of the recording sites and their locations in representative sagittal sections are shown in Fig. 1C. HFVS neurons were observed in all regions of SI (areas 3a, 3b, 1, and 2). The percentage of HFVS neurons was greater in areas 3b and 1 (respectively, 8/151 [5.3%] and 19/354 [5.4%]) than in areas 3a and 2 (respectively, 2/182 [1.1%] and 3/121 [2.5%]). No clear distribution patterns of HFVS neurons were evident within cortical areas.

Activity During Vibratory Cued Trials: Entrained and Non-Entrained Neurons

A prominent feature of the activity of HFVS neurons during vibratory cued trials was the presence of short latency (10-30 ms) vibratory responses that were especially strong at the highest frequency of vibration used (127 Hz). No responses to cue presentation were observed during visually cued trials. In Fig. 2, records are presented for an area 1 HFVS neuron. This neuron was much more responsive to vibratory stimulation at 127 Hz (Fig. 2A-E) than at 27 Hz (Fig. 2A'-E'). The neuron was entrained to the 127 Hz vibratory stimulus. This entrainment is evident in the phase scattergram which shows a concentration of spike occurrences at a particular phase of the vibratory cycle (Fig. 2F). In addition, in the ISI scattergram, bands can be seen that correspond to multiples of the vibratory period (Fig. 2A).

In Fig. 3, records are presented for another area 1 HFVS neuron. The responsiveness of this neuron to 127 Hz vibration (Fig. 3A-E) was greater than its response to 27 Hz vibration (Fig. 3A'-E'). This neuron, however, was not vibration-entrained. Although this neuron responded to 127 Hz vibration with a sustained increase of activity, no signs of entrainment were present in phase rasters (Fig. 3F) nor in the ISI scattergrams (Fig. 3A). The latency of the initial response to the 127 Hz vibratory stimulus was longer for this non-entrained neuron (~28 ms, Fig. 3D) than for the previously illustrated entrained neuron (~ 20 ms, Fig. 2D). The firing rate during vibratory stimulation was less for the non-entrained neuron (Fig. 3B&D) than for the entrained neuron (Fig. 2B&D). Firing rates of both entrained and non-entrained neurons decreased prior to movement onset (at ~ 33 and ~5 ms; Fig. 2D and Fig. 3D, respectively).

Spike Train Analyses

Spike train analyses were performed to distinguish between entrained and non-entrained neurons, and to examine the temporal properties of vibration-entrained activity. In Figs 4A-C and D-F, the results of spike train analyses are presented for the same records as illustrated in Figs 2&3, respectively. Activity epochs from the onset of the vibratory response to 150 ms after vibration onset were used for these analyses. For the vibration-entrained neuron, peaks at multiples of the vibratory period occurred in the ISI histogram (Fig. 4A). Concentrations of ISIs around multiples of the vibratory period also were evident in the joint interval scattergram (Fig. 4B). The cycle distribution for the vibration-entrained neuron showed one preferred phase of the stimulus cycle at which neuronal discharges occurred most frequently (Fig. 4C). For the non-entrained neuron, there were no concentrations of ISIs at multiples of the vibratory period (Fig. 4D), and the cycle distribution was relatively uniform (Fig. 4F).

Figure 4 About Here

The temporal characteristics of entrained responses to vibration differed depending upon the magnitude of vibratory response. In Fig. 5, the results of spike train analyses are presented for three entrained neurons that had different firing rates during 127 Hz vibratory stimulation. One neuron (Fig. 5A-C) had a firing rate of 110 spikes/s. The cycle distribution of this neuron was unimodal (Fig. 5C). The ISI histogram (Fig. 5A) and joint interval scattergram (Fig. 5B) show the presence of ISIs at multiples of the vibratory period, and the presence of short ISIs (less than 5 ms). The ISI clusters in the joint interval scattergram that corresponded to multiples of the vibratory period had characteristic diagonal orientations. Diagonal orientations of the ISI clusters indicated that ISIs which were shorter than the average were likely to be followed by ISIs longer than the average (i.e., ISIs were negatively serially correlated; Perkel et al. 1967). Negative serial correlation of this type typically occurs when neuronal responses to rhythmic driving fluctuate in

time because of synaptic noise (Surmeier and Towe 1987b).

Figure 5 About Here

The two neurons whose records are shown in Fig. 5D-I discharged more often than once per stimulus cycle in response to 127 Hz vibratory stimulation. Their firing rates were 176 and 205 spikes/s, respectively. For these neurons, the proportions of ISIs at multiples of the vibratory period were less, and the proportions of short intervals were more than for the neuron illustrated in Fig. 5A-C. In addition, the joint interval histograms for these neurons contained diagonal bands spanning points (0, T) and (T, 0); where T is the vibratory period (Fig. 5E&D). These bands are indicative of "interrupting" spikes that occurred between responses to rhythmic driving inputs (Surmeier and Towe 1987a; 1987b). For the neuron with the highest firing rate (205 spikes/s), the cycle distribution was bimodal (Fig. 5I). It contained two peaks separated by approximately 180° of phase. Probably, these peaks may indicate responses to both the application and withdrawal of the stimulus (Alloway et al. 1989; Talbot et al. 1968).

The spike trains of non-entrained neurons recorded during vibratory stimulation had unique temporal properties. Most notable were the shapes of ISI distributions and the patterns within the joint interval scattergrams. However, these properties did not reflect any temporal "label" of the vibratory stimulus. In Fig. 6, the results of spike train analyses are presented for three non-entrained neurons. The shapes of ISI distributions and of joint interval histograms varied with the firing rates of the neurons. The two neurons with lesser firing rates had bell shaped ISI distributions (Fig 6A&D; firing rates respectively were 47 and 81 spikes/s). The neuron with the highest firing rate (165 spikes/s) had a Poisson-like ISI distribution (Fig. 6G). No signs of correlations of neuronal discharges with the vibratory stimulus were present in ISI distributions (Fig. 6A,D&G), joint interval scattergrams (Fig. 6B,E&H) or cycle distributions (Fig. 6C,F&I).

Figure 6 About Here

Differences between Entrained and Non-Entrained Neurons

Of the total sample of high-frequency vibratory sensitive neurons, 19/32 were vibration-entrained, and 13/32 were not entrained. The distribution of entrained and non-entrained neurons was not different within and across cortical areas (Fig. 1B&C).

Because the vibration-entrained and non-entrained neurons may belong to different hierarchical stages of information processing (Mountcastle et al. 1969), we compared these two groups of neurons with respect to the latencies of their responses to vibration. We hypothesized that the entrained neurons respond to vibration at shorter latencies because these neurons presumably would be the first recipients of thalamocortical inputs. Analyses of the vibratory response latencies showed that the onset of the vibratory response was, on average, earlier for vibration-entrained neurons than for non-entrained neurons (Table 1). No statistically significant differences in response latency for neurons located in different subdivisions of SI (areas 3a, 3b, 1 and 2) were found. In addition to responding to vibration at shorter latencies, entrained neurons exhibited higher firing rates during the ongoing vibratory stimulation than non-entrained neurons (Table 1).

Table 1 About Here

Premovement Changes in Activity

During both vibratory and visually-cued trials, firing rates of HFVS neurons changed prior to movement onsets. During 127 Hz vibratory cued trials, premovement changes in activity were detected for 20/32 neurons for flexion movements and for 21/32 neurons for extension movements. For 18 neurons, records also were obtained during visually cued trials. Premovement changes were observed for 16/18 neurons for visually cued flexions and for 15/18 neurons for extensions. In Fig. 7, the activity patterns of an area 1 neuron are illustrated that were exhibited during vibratory and visually cued wrist flexions. This neuron had a RF located on the thenar eminence. The firing rate of this neuron decreased at ~100 ms prior to movement onset during vibratory-cued trials. However, during visually-cued trials, the neuron's firing rate increased at ~140 ms prior to movement onset. For vibratory-cued trials, premovement decreases in firing rate more often were observed (29/40 instances; Fig. 8A), whereas firing rate increases typically occurred during visually-cued trials (27/31 instances; Fig. 8B). The type of activity change was not dependent upon movement direction.

Figure 7 About Here

The onsets of premovement activity for HFVS neurons were compared with the EMG onsets for different forearm muscles for two of the monkeys (Nelson 1987; Lebedev et al. 1994). EMG onsets provided estimates of the probable time of arrival of movement-related peripheral activity in SI. A minimal peripheral conduction time of 11 ms was subtracted from the EMG onsets (Wiesendanger and Miles 1982), thus the earliest EMG onset was ~100 ms prior to movement onset. The average onset of EMG activity changes was 60 ms prior to movement onset. Most (~80%) of the premovement activity changes of HFVS neurons occurred after the earliest EMG onset. Approximately 60% occurred after the average onset.

Figure 8 About Here

Discussion

We examined the activity of high-frequency vibratory sensitive (HFVS) neurons located in monkey SI during the performance of vibratory-cued and visually-cued hand movements. The small proportion of HFVS neurons (~4%) that we observed is consistent with the results of previous studies. Mountcastle et al. (1969) reported that only about 6% of SI neurons belonged to the Pacinian class. The relative number of HFVS neurons in SI is comparable with the proportion of Pacinian fibers in peripheral nerves (~9 %; Talbot et al. 1968). HFVS neurons more frequently were observed in areas 3b and 1 than in areas 3a and 2, perhaps because areas 3b and 1 receive more inputs from cutaneous and subcutaneous afferents than areas 3a and 2 that receive inputs mostly from muscle and joint afferents (Jones 1986; Kaas 1993).

HFVS neurons were split into two groups based on the presence or absence of correlation between the neuronal activity and the temporal characteristics of the vibratory stimulus. The neurons of the first group preferentially discharged at a particular phase of the stimulus cycle. For

these vibration-entrained neurons, ISIs at multiples of the vibratory period frequently were observed. Moreover, negative serial correlations were detected for ISI clusters in joint interval scattergrams. These negative correlations occurred, in some cases, because of non-precise time-locking of neuronal discharges to the stimulus and, in other cases, because of the presence of "interrupting" spikes at less than the modal interval (Surmeier and Towe 1987a; 1987b). For the second group of HFVS neurons (non-entrained neurons), temporal correlations of the discharges with the stimulus were not evident.

The activity of vibration-entrained and non-entrained HFVS neurons previously has been described (Ferrington and Rowe 1980; Mountcastle et al. 1969). In these studies, it was suggested that entrained neurons are the major targets of thalamocortical projections, and may be stellate neurons of cortical layers 3 and 4. Furthermore, it was suggested that non-entrained neurons probably are pyramidal cells that receive inputs from the entrained neurons. During transmission of vibration-related activity and its integration with other inputs, the fine temporal characteristics of vibratory signals may become obscured. Our data are consistent with the suggestion that information flows from entrained to non-entrained neurons. Indeed, the latency of the vibratory response was shorter for entrained neurons. Therefore, these neurons may receive thalamocortical signals first and then transmit them to non-entrained neurons.

Mountcastle et al. (1969) suggested that Pacinian information may be encoded differently by entrained and non-entrained neurons. For entrained neurons, the fine temporal structure of spike trains appears to encode the frequency and amplitude characteristics of the vibratory stimulus. From our observations, several encoding principles may be suggested for entrained neurons. Spike periodicity may encode the stimulus frequency (Mountcastle et al. 1969). The stimulus amplitude may be indicated by the relative number of ISIs around one or more vibratory periods. Thus, with decreases of stimulus amplitude, more ISIs may occur around multiples of the vibratory period as compared with the number of ISIs around a single vibratory period. In addition, short ISIs (< 5ms) may contribute to the encoding of stimulus amplitude. Spikes that are separated by short ISIs may produce stronger effects at postsynaptic sites than those separated by long ISIs because of temporal summation of PSPs (Eccles 1964). The encoding principles for non-entrained neurons remain unclear. Spike trains of non-entrained neurons have unique temporal characteristics. However, no clear relationship was evident between these characteristics and the temporal properties of vibratory stimuli.

The activity of HFVS neurons changed prior to movement onset. Premovement changes in somatosensory cortical activity previously have been reported (Chapin and Woodward 1982; Evarts 1972; Fromm and Evarts 1982; Lamarre et al. 1983; Lebedev et al. 1994; Nelson 1987; 1988; Nelson and Douglas 1989; Nelson et al. 1991; Shin and Chapin 1990; Soso and Fetz 1980). It is believed that activity changes that precede EMG onset probably have central rather than peripheral origins. For HFVS neurons, onsets of premovement activity preceded the earliest EMG onset in only 20% of the cases. For these cases, the signals of central origin may have modulated the neuronal activity prior to voluntary movements.

Premovement patterns of activity were different during vibratory-cued as compared with visually-cued trials. During vibratory-cued trials, premovement decreases in firing rate were observed most often. During visually-cued trials, firing rates typically increased prior to movements. This can be contrasted with the pattern of premovement activity of quickly adapting (QA) SI neurons (Nelson et al. 1991). For QA neurons, premovement increases in firing rate

occurred for both vibratory and visually-cued trials. Moreover, these increases were greater for vibratory-cued trials, probably because of the summation of premovement and stimulus-related components of activity (Nelson et al. 1991). We suggest that the role of premovement activity may be different for HFVS neurons than for QA neurons. It seems unlikely that premovement changes in activity of HFVS neurons result primarily from the interaction of peripheral signals. If these effects were solely of peripheral origin, movement-related activity changes during visually-cued trials would be likely to induce similar activity changes during vibratory-cued trials. An intriguing explanation for premovement activity decreases during vibratory-cued trials is that these decreases occurred because of gating of Pacinian inputs. Pacinian input is undoubtedly important in this experimental paradigm for initial go-cue detection. However, for movement execution, strong vibratory input transmitted by the Pacinian channel may not be as important or even it may conflict with feedback information about the movement (Nelson et al. 1991). Therefore, it may be necessary to suppress this input prior to movement onset.

Acknowledgments

We thank J. M. Denton and for technical assistance. This work was supported by United States Air Force Grant AFOSR 91-0333 to R. J. Nelson.

References

Alloway KD, Sinclair RJ, Burton H (1988) Responses of neurons in somatosensory cortical area II of cats to high-frequency vibratory stimuli during iontophoresis of GABA antagonist and glutamate. Somatosensory and Motor Res 6: 109-140

Burton H, Sinclair RJ (1991) Second somatosensory cortical area in macaque monkeys: 2. Neuronal responses to punctate vibrotactile stimulation of glabrous skin on the hand. Brain Res 538: 127-135

Cauna N, Mannan G (1958) The structure of human digital pacinian corpuscles (corpuscula lamellosa) and its functional significance. J Anat 92: 1-20

Chapin JK, Woodward DJ (1982) Somatic sensory transmission to the cortex during movement: gating of single cell responses to touch. Exp Neurol 78: 654-669

Colburn TR, Evarts EV (1978) Long-loop adjustments during intended movements: Use of brushless DC torque motors in studies of neuromuscular function. In: Desmedt JE (ed) Progress in Clinical Neurophysiology, Vol 4. Karger, New York, pp 153-166

Eccles JC (1964) The Physiology of Synapses. Berlin: Springer.

Ellaway PH (1977) An application of cumulative sum technique (cusums) to neurophysiology. J Physiol (Lond) 265: 1-2P

Evarts EV (1966) Methods for recording activity of individual neurons in moving animals. In: Rushmer RF (ed) Methods in Medical Research. Vol II. Yearbook, Chicago, pp 241-250.

Evarts EV (1972) Contrasts between activity of precentral and postcentral neurons of cerebral cortex during movement in the monkey. Brain Res 40: 25-31

Ferrington DG, Rowe M (1980) Differential contribution to coding of cutaneous vibratory information by cortical somatosensory areas I and II. J Neurophysiol 43: 310-331

Fromm C, Evarts EV (1982) Pyramidal tract neurons in somatosensory cortex: central and peripheral inputs during voluntary movement. Brain Res 238: 186-191

Jiang W, Chapman CE, Lamarre Y (1991) Modulation of the cutaneous responsiveness of neurons in the primary somatosensory cortex during conditioned arm movements in the monkey. Exp Brain Res 84: 342-354

Jones EG (1986) Connectivity of the primate sensory-motor cortex. In: Jones EG, Peters A (eds) Cerebral Cortex. Volume 5. Sensory-Motor Areas and Aspects of Cortical Connectivity. Plenum Press, pp 113-183

Kaas JH (1993) The functional organization of somatosensory cortex in primates. Ann Anat 175: 509-518

Kumamoto K, Senuma H, Ebara S, Matsuura T (1993) Distribution of pacinian corpuscles in the hand of the monkey, Macaca fuscata. J Anat (England) 183: 149-154

Lamarre Y, Spidalieri G, Chapman CE (1983) A comparison of neuronal discharge recorded in the sensori-motor cortex, parietal cortex and dentate nucleus of the monkey during arm movements triggered by light, sound or somesthetic stimuli. In: Massion J, Paillard J, Schultz W, Wiesendanger M (eds). ExpBrain Res Suppl 7: Neural Coding of Motor Performance. Berlin-Heidelberg: Springer-Verlag, pp 141-157

Lebedev MA, Denton JM, Nelson RJ (1994) Vibration-entrained and premovement activity in monkey primary somatosensory cortex. J Neurophysiol 72: 1654-1673.

Lebedev MA, Nelson RJ (1994) Two types of vibratory responsive Pacinian-like neurons in monkey primary somatosensory cortex (SI) studied during active hand movements. (567.16). Soc for Neurosci Abstr 20: 1388

Lemon R (1984) Methods for Neuronal Recording in Conscious Animals. IBRO Handbook Series: Methods in the Neurosciences. Vol 4. John Wiley & Sons, Chichester, UK

Mountcastle VB, Talbot WH, Sakata H, Hyvärinen J (1969) Cortical neuronal mechanisms in flutter-vibration studies in unanesthetized monkeys: Neuronal periodicity and frequency discrimination. J Neurophysiol 32: 452-484

Mountcastle VB, Steinmetz MA, Romo R (1990) Frequency discrimination in the sense of flutter: Psychophysical measurements correlated with postcentral events in behaving monkeys. J Neurosci 10: 3032-3044

Nelson RJ (1987) Activity of monkey primary somatosensory cortical neurons changes prior to active movement. Brain Res 406: 402-407

Nelson RJ (1988) Set related and premovement related activity of primate somatosensory cortical neurons depends upon stimulus modality and subsequent movement. Brain Res Bull 21:411-424

Nelson RJ, Douglas VD (1989) Changes in premovement activity in primary somatosensory cortex differ when monkeys make hand movements in response to visual vs vibratory cues. Brain Res 484: 43-56

Nelson RJ, Smith BN, Douglas VD (1991) Relationship between sensory responsiveness and premovement activity of quickly adapting neurons in areas 3b and 1 of monkey primary somatosensory cortex. Exp Brain Res 84: 75-90

Perkel DH, Gerstein G, Moore G (1967) Neuronal spike trains and stochastic point processes. I. The single spike train. Biophys J 7: 391-418

Poggio T, Viernstein L (1964) Time series analysis of impulse sequences of thalamic somatic sensory neurons. J Neurophysiol 27: 517-545

Quilliam TA (1966) Structure of receptor organs. In: Reuck, A.V.S., Knight, J. (eds). Touch, Heat and Pain. London: J.&A. Churchill.

Rodieck RW, Kiang NY-S, Gerstein GL (1962) Some quantitative methods for the study of spontaneous activity of single neurons. Biophys J 2: 351-368

Sato K (1957) On the sensory innervation of the palm and sole of Formosan Macaque. Archivum Histologicum Japonicum 17: 1-22

Sato M (1961) Responses of Pacinian corpuscles to sinusoidal vibration. J Physiol 159: 391

Shin HC, Chapin JK (1990) Movement induced modulation of afferent transmission to single neurons in the ventroposterior thalamus and somatosensory cortex in rat. Exp Brain Res 81: 515-522

Siebler M, Köller H, Rose G, Müller HW (1991) An improved graphical method for pattern recognition from spike trains of spontaneously active neurons. Exp Brain Res 90: 141-146

Soso MJ, Fetz EE (1980) Responses of identified cells in postcentral cortex of awake monkeys during comparable active and passive joint movements. J Neurophysiol 43: 1090-1110

Surmeier DJ, Towe AL (1987a) Properties of proprioceptive neurons in the cuneate nucleus of the cat. J Neurophysiol 57: 938-961

Surmeier DJ, Towe AL (1987b) Intrinsic features contributing to spike train patterning in proprioceptive cuneate neurons. J Neurophysiol 57: 962-976

Talbot WH, Darian-Smith I, Kornhuber HH, Mountcastle VB (1968) The sense of flutter-vibration: Comparison of the human capacity with response patterns of mechanoreceptive afferents from the monkey hand. J Neurophysiol 31: 301-334

Vaadia E, Kurata K, Wise SP (1988) Neuronal activity preceding directional and nondirectional cues in the premotor cortex of rhesus monkeys. Somatosensory and Motor Res 6: 207-230

Wall PD, Cronly-Dilon JR (1960) Pain, itch and vibration. Am Med Assoc Arch Neurol 2: 365-375

Wiesendanger M, Miles TS (1982) Ascending pathway of low-threshold muscle afferents to the cerebral cortex and its possible role in motor control. Physiol Rev 62: 1234-1270

Table 1. Characteristics of activity during the hold period and of vibratory responses.

	Vibration-Entrained Neurons (n = 19)	Non-Entrained Neurons (n=13)	Statistical Comparisons
Firing Rate (spike / s)			
Hold Period	19.62 ± 9.98	15.75 ± 13.30	n. s.
27 Hz Vibration	91.16 ± 54.76	55.60 ± 56.79	$p < 0.05$
57 Hz Vibration	88.29 ± 29.80	50.59 ± 30.32	$p < 0.005$
127 Hz Vibration	122.74 ± 40.25	84.30 ± 44. 39	$p < 0.02$
Response Latency (ms)			
27 Hz Vibration	19.74 ± 3.78	23.00 ± 7.56	n. s.
57 Hz Vibration	18.97 ± 6.21	24.73 ± 7.79	$p < 0.05$
127 Hz Vibration	17.60 ± 4.29	23.92 ± 7.53	$p < 0.05$

Values indicate mean ± standard deviation. Significance levels indicated are for both one-factor ANOVA with the Scheffé comparison test and Mann-Whitney *U*-test. Firing rate during the hold period was calculated from the number of spikes counted for the 500 ms epoch preceding vibration onset. Firing rate for the vibratory response was calculated from the number of spikes occurring between onset of the vibratory response and 150 ms after vibration onset.

Figure Legends

Figure 1. Cortical locations of high-frequency vibratory sensitive neurons. A: A drawing of a dorsolateral view of the brain. CS - central sulcus; IPS - intraparietal sulcus. B: A table showing the number of vibration-entrained and non-entrained neurons recorded in areas 3a, 3b, 1 and 2. C: Locations of recording sites for four monkeys (surface maps of electrode penetrations and representative sagittal sections through the cortex showing the neurons' locations).

Figure 2. Records for a vibration-entrained area 1 neuron. A-F: Vibrotactile stimulation at 127 Hz; A'-E': at 27 Hz. Left halves of panels - displays centered on vibration onset; right halves - on movement onset. Onsets of movement and vibration are at the zero, respectively. A&A': Displays of interspike intervals. B&B': Histograms of activity (bin width is 5 ms). C&C': Raster displays of activity. Trials are ordered by reaction time. D&D': Average (normalized by the number of trials) cumulative sums (CUSUMs). Significant changes of the slope are marked. Values represent onsets of activity changes. Negative values are before centering event; positive values indicate occurrence after event. E&E': Average position traces. F: Displays of spike occurrences relative to the stimulus phase. G: Receptive field (RF) schematics. This neuron had a cutaneous RF located on the hypothenar eminence. H: Schematics of the neuron's cortical location.

Figure 3. Records for a non-entrained area 1 neuron. Conventions as in Fig. 2. A-F: vibrotactile stimulation at 127 Hz; A'-E': at 27 Hz. Responsiveness to vibration was greater at 127 Hz than at 27 Hz (B&B'). Response latency was 28.5 ms at 127 Hz (D) and 25.6 ms at 27 Hz (D'). G: Receptive field (RF) schematics. This neuron had a cutaneous RF located on the fourth digit. H: Schematics of the neuron's cortical location.

Figure 4. Spike train analyses of neuronal responses to vibration. Vibratory frequency was 127 Hz. A-C: Analyses of records of an entrained neuron (Fig. 2), and D-F: of a non-entrained neuron (Fig. 3). A&D: Distributions of inter-spike intervals (ISIs). B&E: Joint interval scattergrams. C&F: Cycle distributions.

Figure 5. Spike train analyses for three neurons entrained to vibration at 127 Hz. Conventions as in Fig. 4.

Figure 6. Spike train analyses for three neurons that were responsive but not entrained to the 127 Hz vibration. Conventions as in Figs 4&5.

Figure 7. Records of activity of an area 1 neuron during vibratory and visually cued trials. Conventions as in Fig. 2. A-F: vibratory-cued trials (127 Hz); A'-E': visually-cued trials. G: Receptive field (RF) schematics. This neuron had a cutaneous RF located on the thenar eminence. H: Schematics of the neuron's cortical location.

Figure 8. Frequency distribution histograms of premovement activity onsets for vibratory-cued (A) and visually-cued (B) trials.

A.

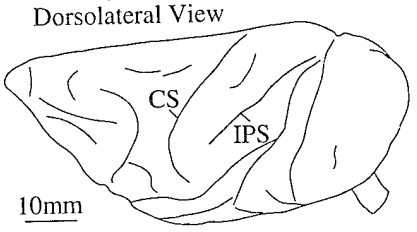

B.

Cortical Area

	3a	3b	1	2	Total
• Entrained	2	4	11	2	19
○ Non-Entrained	0	4	8	1	13
Total	2	8	19	3	32

C.

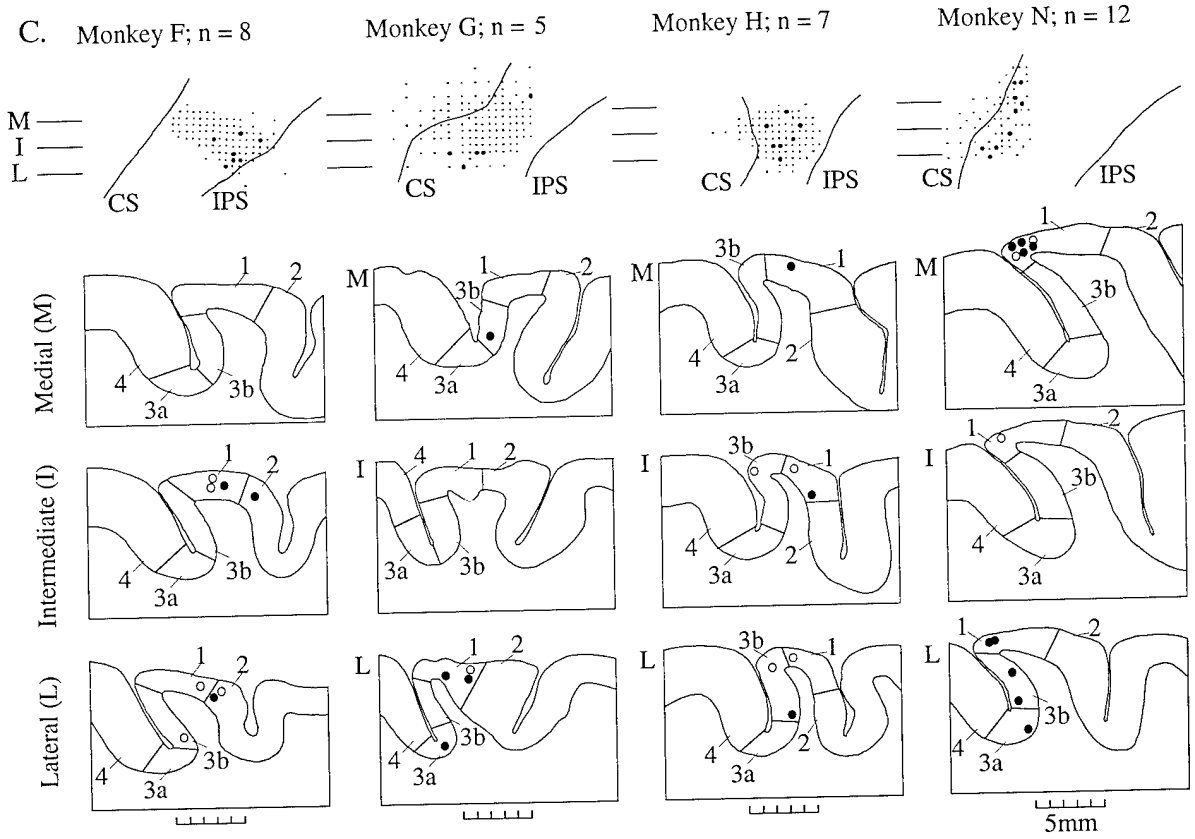

Figure 1

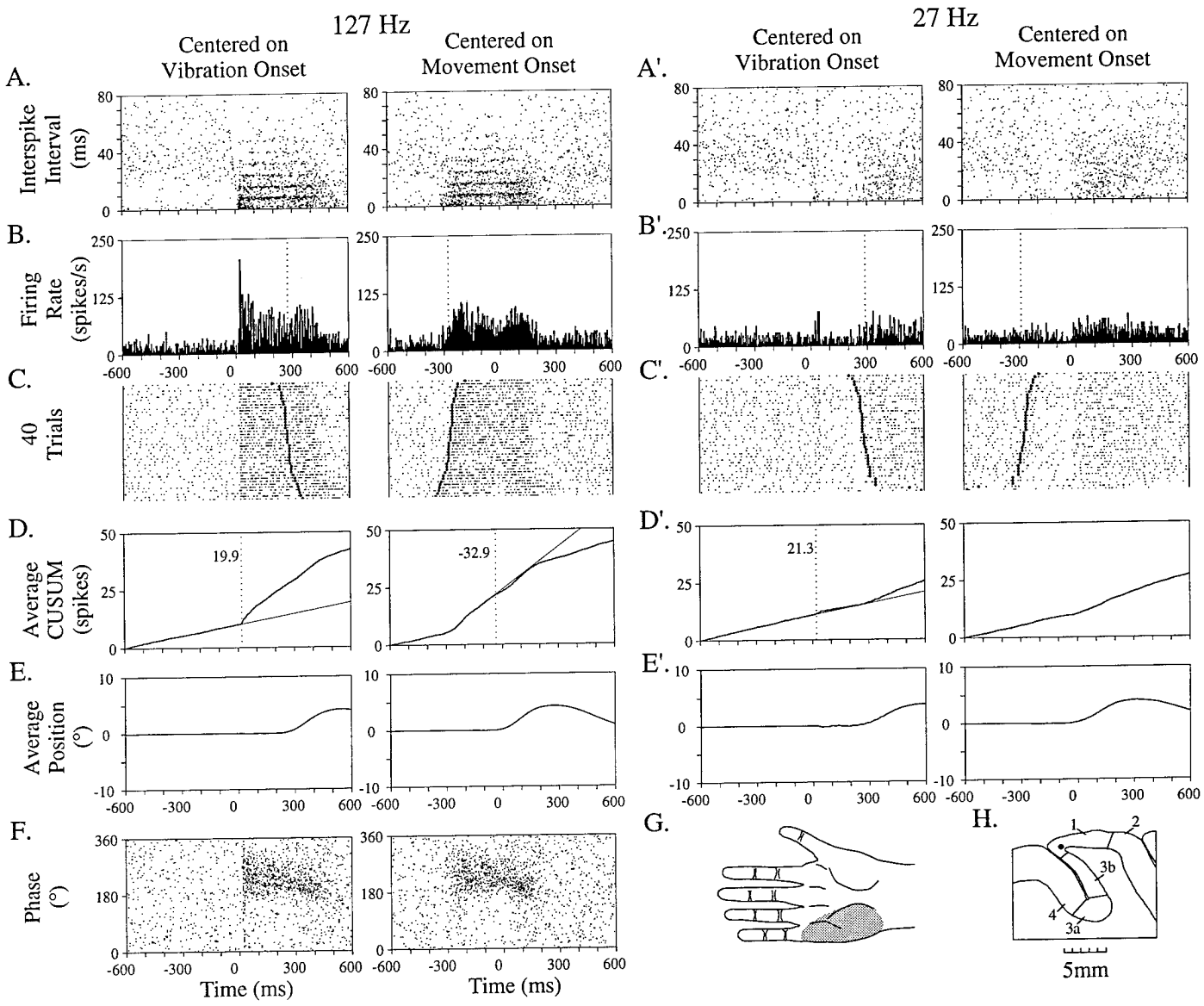
127 Hz
27 Hz
Centered on Vibration Onset
Centered on Movement Onset
A.
A'.
B.
B'.
C.
C'.
D.
D'.
E.
E'.
F.
G.
H.
Interspike Interval (ms)
Firing Rate (spikes/s)
40 Trials
Average CUSUM (spikes)
Average Position (°)
Phase (°)
19.9
-32.9
21.3
Time (ms)
1
2
3b
4
3a
5mm

Figure 2

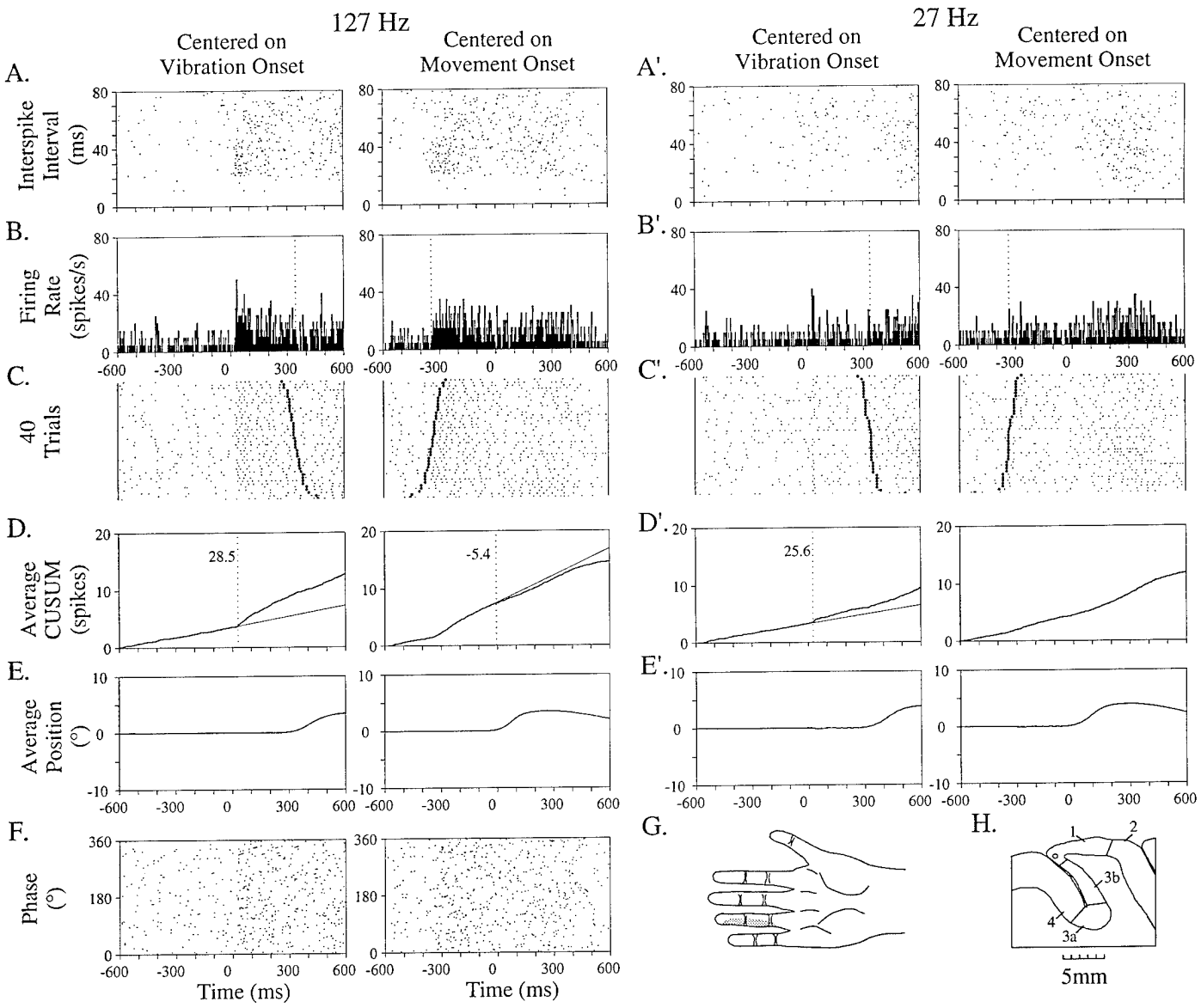
127 Hz
27 Hz
Centered on Vibration Onset
Centered on Movement Onset
A.
A'.
B.
B'.
C.
C'.
D.
D'.
E.
E'.
F.
G.
H.
Interspike Interval (ms)
Firing Rate (spikes/s)
40 Trials
Average CUSUM (spikes)
Average Position (°)
Phase (°)
28.5
-5.4
25.6
Time (ms)
1
2
3b
4
3a
5mm

Figure 3

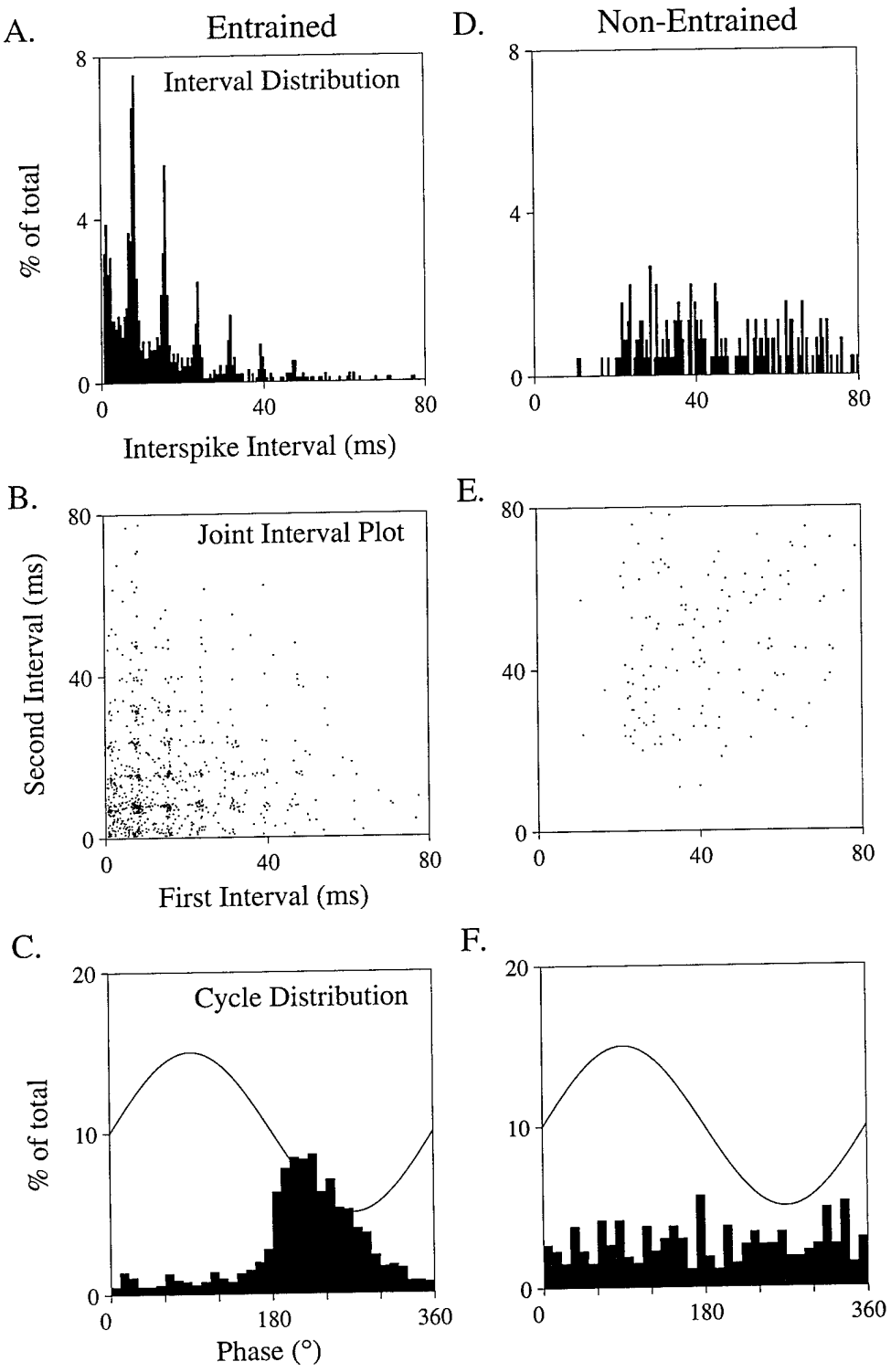
A.
Entrained
Interval Distribution
% of total
8
4
0
0
40
80
Interspike Interval (ms)
D.
Non-Entrained
8
4
0
0
40
80
B.
Joint Interval Plot
Second Interval (ms)
80
40
0
0
40
80
First Interval (ms)
E.
80
40
0
0
40
80
C.
Cycle Distribution
% of total
20
10
0
0
180
360
Phase (°)
F.
20
10
0
0
180
360

Figure 4

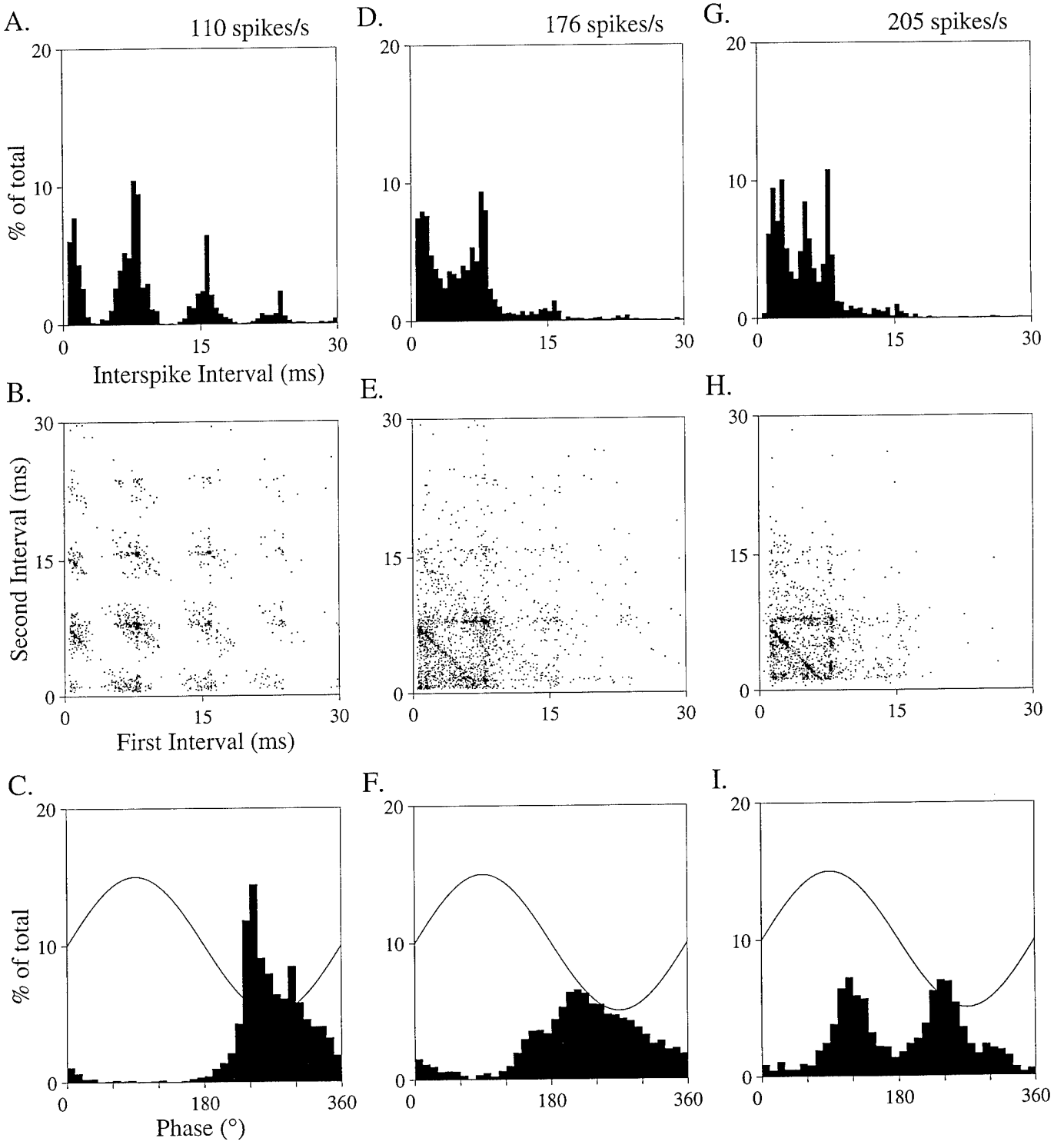
A.
110 spikes/s
D.
176 spikes/s
G.
205 spikes/s
% of total
Interspike Interval (ms)
B.
E.
H.
Second Interval (ms)
First Interval (ms)
C.
F.
I.
% of total
Phase (°)

Figure 5

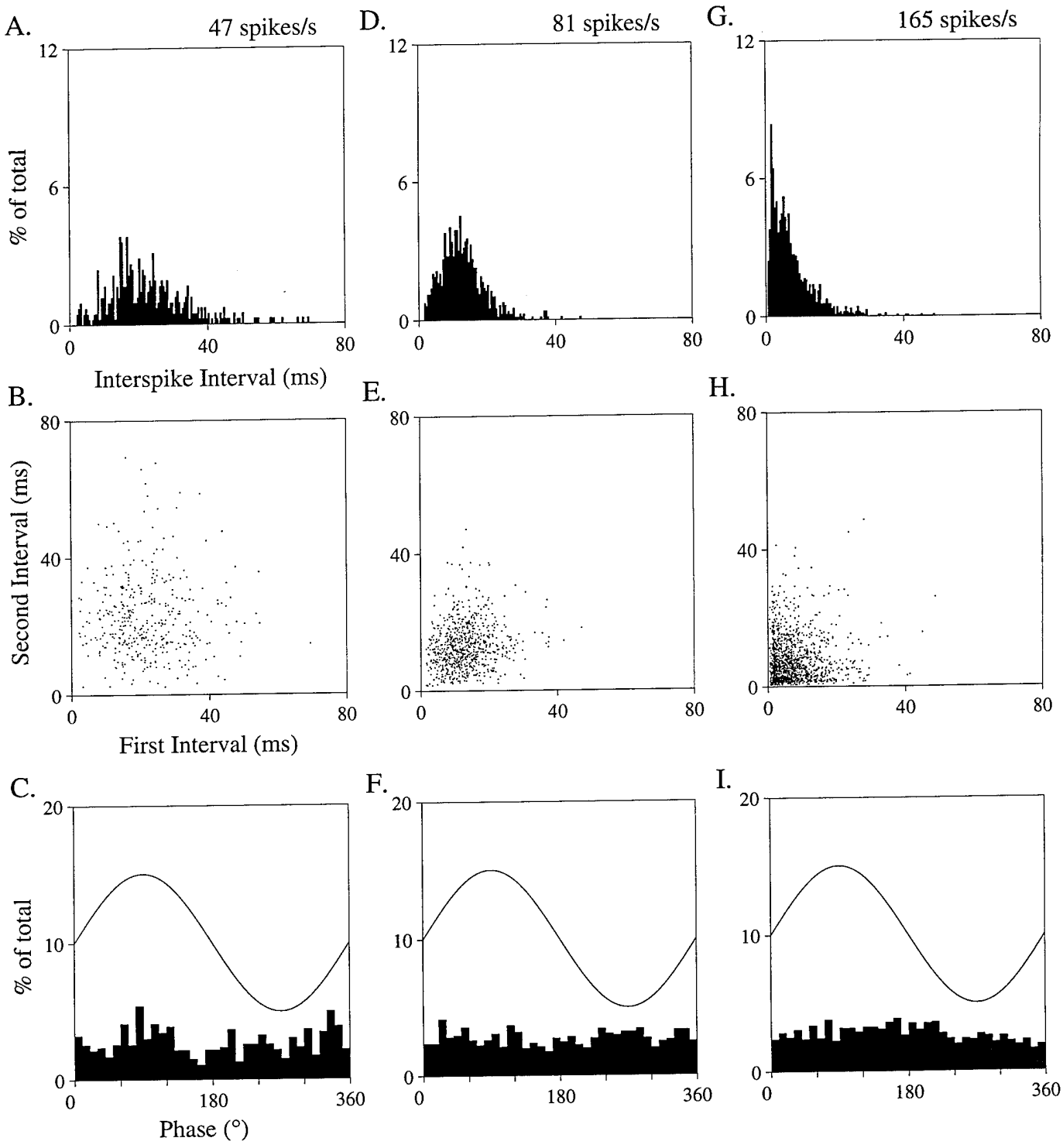
A.
47 spikes/s
D.
81 spikes/s
G.
165 spikes/s
% of total
Interspike Interval (ms)
B.
E.
H.
Second Interval (ms)
First Interval (ms)
C.
F.
I.
% of total
Phase (°)

Figure 6

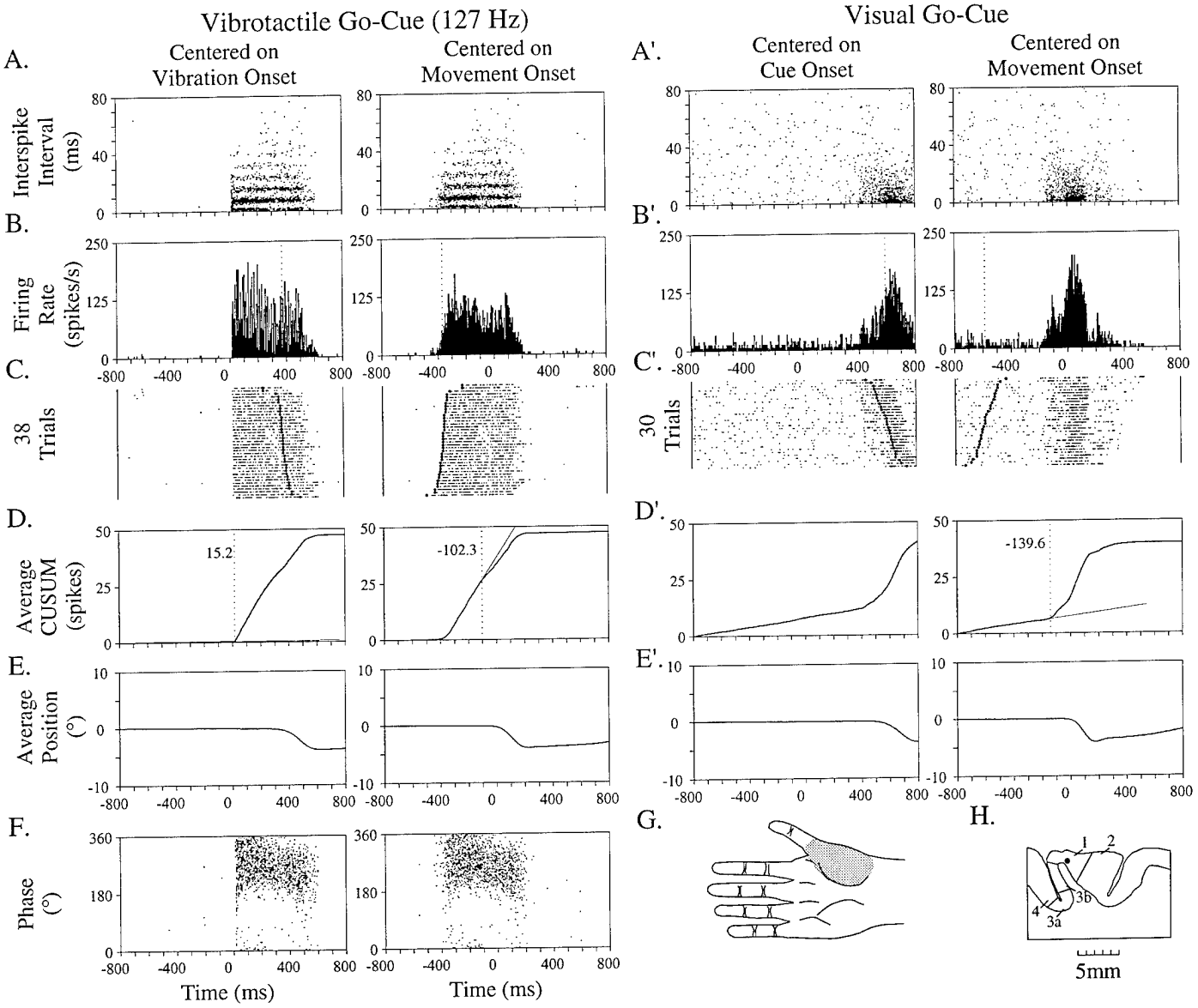
Vibrotactile Go-Cue (127 Hz)
Visual Go-Cue
A.
A'.
Centered on Vibration Onset
Centered on Movement Onset
Centered on Cue Onset
Centered on Movement Onset
Interspike Interval (ms)
B.
B'.
Firing Rate (spikes/s)
C.
C'.
38 Trials
30 Trials
D.
D'.
Average CUSUM (spikes)
15.2
-102.3
-139.6
E.
E'.
Average Position (°)
F.
Phase (°)
Time (ms)
Time (ms)
G.
H.
1
2
3b
3a
4
5mm

Figure 7

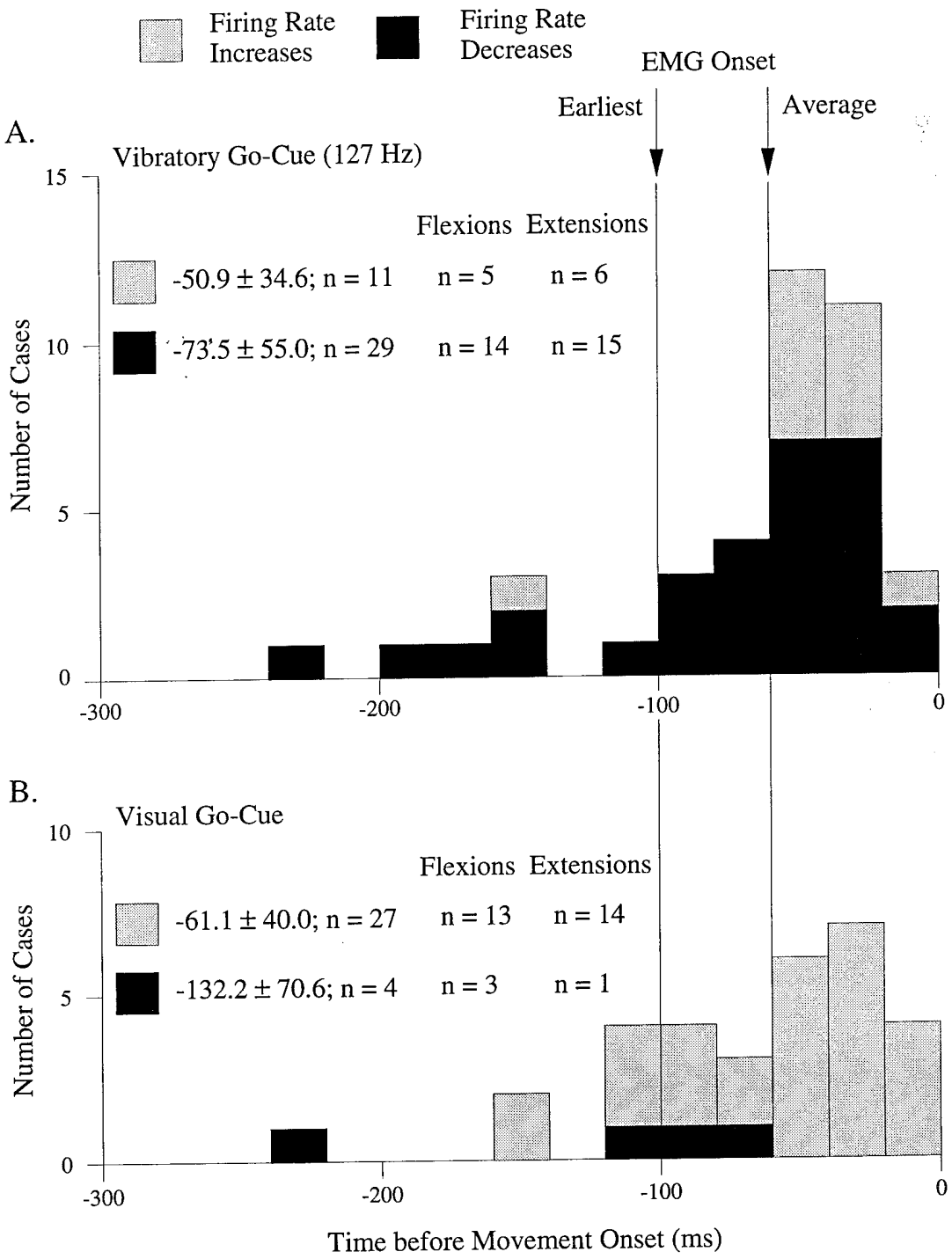
Firing Rate Increases
Firing Rate Decreases
EMG Onset
Earliest
Average
A.
Vibratory Go-Cue (127 Hz)
Flexions Extensions
-50.9 ± 34.6; n = 11 n = 5 n = 6
-73.5 ± 55.0; n = 29 n = 14 n = 15
Number of Cases
15
10
5
0
-300
-200
-100
0
B.
Visual Go-Cue
Flexions Extensions
-61.1 ± 40.0; n = 27 n = 13 n = 14
-132.2 ± 70.6; n = 4 n = 3 n = 1
Number of Cases
10
5
0
-300
-200
-100
0
Time before Movement Onset (ms)

Figure 8